

Fracture Mechanics of Concrete Structures  
**Proceedings FRAMCOS-3**  
AEDIFICATIO Publishers, D-79104 Freiburg, Germany

## **LOAD CARRYING CAPACITY OF BEAMS USING FIBRES AS SHEAR REINFORCEMENT**

K. Noghabai, T. Olofsson  
Luleå University of Technology, Division of Structural Engineering  
Sweden

### **Abstract**

The load bearing capacity of reinforced beams of fibrous high-strength concrete is investigated, experimentally and computationally. Both metallic (steel) and non-metallic (polyolefin and carbon) fibres are used, keeping the volume fraction to 1%. A nonlinear truss model is outlined which incorporates most of the pertinent mechanisms in the experiments, including the rebar-to-concrete bond and crack widths. The law for evolution of stable growth of local cracks in the structure is based on the response of uniaxial tensile tests.

**Key words:** Shear capacity, Steel fibres, Non-metallic fibres, High-strength concrete, Uniaxial tensile test.

### **1 Introduction**

In order to remedy the brittle performance of some high-strength concrete (HSC) structures, fibres can be added to the concrete matrix. After initia-

tion of cracks, the crack-arresting effect of fibres provides a redistribution of stresses within the structure and consequently the overall structural toughness may be enhanced. Another major - and primarily industrial - incentive in using fibres is to reduce the production cost by, where possible, avoiding conventional reinforcement bars. Hence, the practical implication of this study is to see if stirrups may be avoided in beams. Still, two main factors discourage use of fibres in concrete, the current high cost of fibres but perhaps most importantly the lack of rules and guidelines for design of structures of fibre reinforced concrete. Since the cost of fibres and also issues concerning feasibility hinder a lavish use of fibres, the design tools (models) must consider how the fibrous concrete should be composed in order to fulfil the functional requirements put on the structure. Thus, the models must be able to foresee the mechanisms of failure in the structures. Such a model is devised here for reinforced concrete beam in flexure. The model prediction is compared with experimental results.

## 2 Experiments

### 2.1 Concrete composition and types of fibres

The experimental program involved two series of tests. In the first test series only HSC was used whereas in the second test series also specimens of normal-strength concrete (NSC) were cast. The recipe of the concretes are given in Table 1. Both metallic and non-metallic fibres are used in NSC- as well as HSC-mixtures. Based on the cost and feasibility aspects mentioned in the introduction, the volume fraction of the fibres in all batches of fibrous concrete is set to approximately 1%. In order to distinguish the different batches or specimens in the text, the following notation will be used. For fibrous concrete, the type of fibres used in the batch is given as subscript index. The fibres are typified by their materials according to "S" for steel, "P" for polyolefin and "Carbon" for carbon fibres. The different types of steel and polyolefin fibres are distinguished as the initials S and P are followed by the fibre dimensions. For instance, a steel fibre of length  $l_f = 35$  mm and a diameter  $\varnothing_f = 0.6$  mm is denoted S35/0.6. For the non-fibrous case the subscript index REF is used. In some batches the two types of steel fibres were combined to an equal amount ( $40 \text{ kg/m}^3$  of S30/0.6 and S6/0.15 respectively). These batches are denoted HSC<sub>Smix</sub> or NSC<sub>Smix</sub>. The configuration and other informations on the chosen fibres are given in Noghabai and Olofsson (1998).

Table 1: Concrete recipes. Dry weights of materials in kg/m<sup>3</sup>

| Batch | Sand   |         | Coarse aggregate |     | Cement | Silica fume | Super-plasticizer | Water |
|-------|--------|---------|------------------|-----|--------|-------------|-------------------|-------|
|       | 0-8 mm | 8-12 mm | 12-16 mm         |     |        |             |                   |       |
| NSC   | 919    | 552     | 572              | 350 | -      | -           | 178               |       |
| HSC   | 730    | -       | 1152             | 490 | 48     | 4.62        | 166               |       |

## 2.2 Beam specimens and experimental set-up

Both test series are based on a three-point bending procedure on beams according to Fig. 1. All beams were provided with bending reinforcement in order to avoid a flexural failure (or steel yielding) during the tests. Considerations were paid to the detailing of the rebars with respect to the concrete cover and sufficient anchorage at the ends of the beams. Beams of NSC (with and without fibres) were used in the second test series only. In both test series, two beams were made from batches of plain concrete, of which one was reinforced with stirrups.

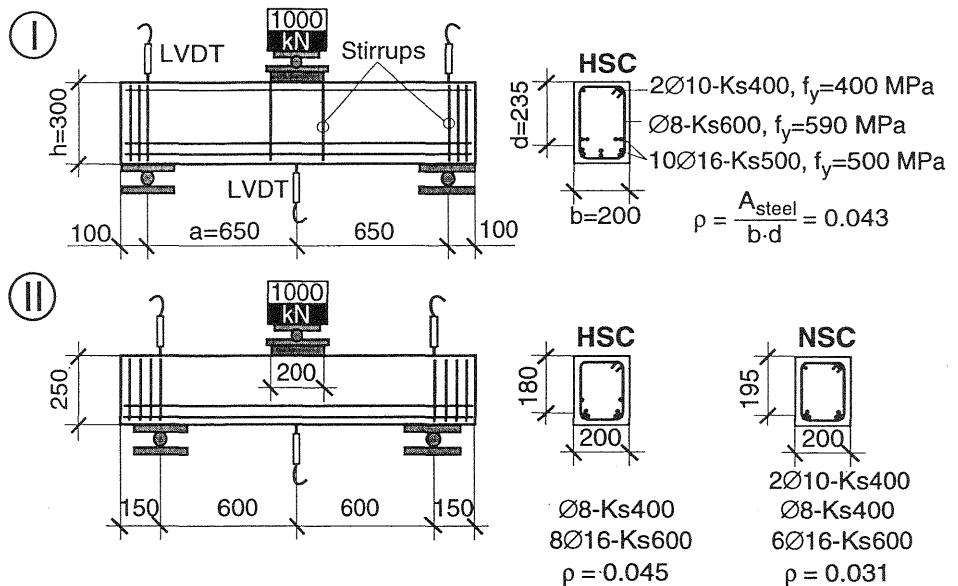


Fig. 1. Beams and experimental setup for test series I and II.

For the sake of convenience the non-fibrous beams without shear reinforcement are indexed by REF whereas the specimens with shear reinforcement are marked by the dimension and spacing of the stirrups. The beams of the two test series are distinguished by giving the number of the test series elevated in roman type.

The tests were performed in displacement control via LVDTs. The rate of displacement was set to 0.01-0.02 mm/second. The control was based on the mid-deflection of the beams. The load was applied by hydraulic jacks with a capacity of 1000 kN. Both supports were free to slide horizontally while the beam was fixed laterally at the load application point.

### 2.3 Structural behaviour

In Fig. 2 the experimental load versus mid-point deflection curves are given. For the reference cases the first peaks on the curves correspond to formation of the oblique cracks. This behaviour is absent in the fibrous beams due to a strain redistribution that evens out the stresses along the two diagonal cracks. This resembles the case of beams reinforced with stirrups. However, the failure phenomena for beams of fibrous concrete often distinguish themselves by a crack patterns with less branching-offs and smaller crack widths. Consequently, for steel fibre reinforced concretes the structural response is stiffer. A compression failure limits the capacity of beams  $HSC^I_{Smix}$ ,  $HSC^{II}_{S6/0.15}$  and  $HSC^{II}_{Smix}$  and since fibres have virtually no bearing on the properties of concrete in compression, the collapse is always sudden. One could say that by adding fibres the redistribution of stresses that takes place in the beams enables use of the high compressive strength of the concrete. By comparing the different responses of  $HSC^I_{S6/0.15}$  and  $HSC^{II}_{S6/0.15}$  in Fig. 2 it is clear that the amount of fibres must be varied for beams of various dimensions in order to obtain not only a high load carrying capacity but also toughness in post-failure stage.

The ascending load-deflection responses in Fig. 2 assert a stable growth of local cracks (flexural as well as oblique ones). A size effect is decisive for the stability in propagation of each local crack, but the collapse of a beam is caused by a global, structural instability. Apparently, this global instability may depend on different mechanisms. They may be categorized as failure in the compression zone, tensile zone or in the web. The failure in the tensile zone is associated with bond failure and is manifested by spalling of the concrete cover. It can be caused by a lack of sufficient anchorage at the supports or, due to large deformations in the rebars (as a

consequence of Poisson's effect on the rebar for strains corresponding to its yielding) or, a so-called "dowel action" associated with large beam deflections. It is reasonable to assume that, as long as the response curve is rising, the stable cracks are active in Mode I only. Thus, also the diagonal "shear" cracks are viewed as a fracture in the principal direction. A possible sliding motion along the oblique crack plane (Mode II) requires that the crack is under severe lateral confinement. A constitutive law that governs the progress of the local cracks must be defined. This may be based on the responses of a concrete specimen subjected to a Mode I failure. The results of such direct, uniaxial tensile tests on specimens made from the concrete used in test series I, are presented in Noghabai and Olofsson (1998). The similitude in the responses of  $HSC^I_{Carbon}$  and  $HSC^I_{REF}$  in Mode I obtained by such a direct test are reflected in the almost identical beam responses in Fig. 2. This is in line with the statements above.

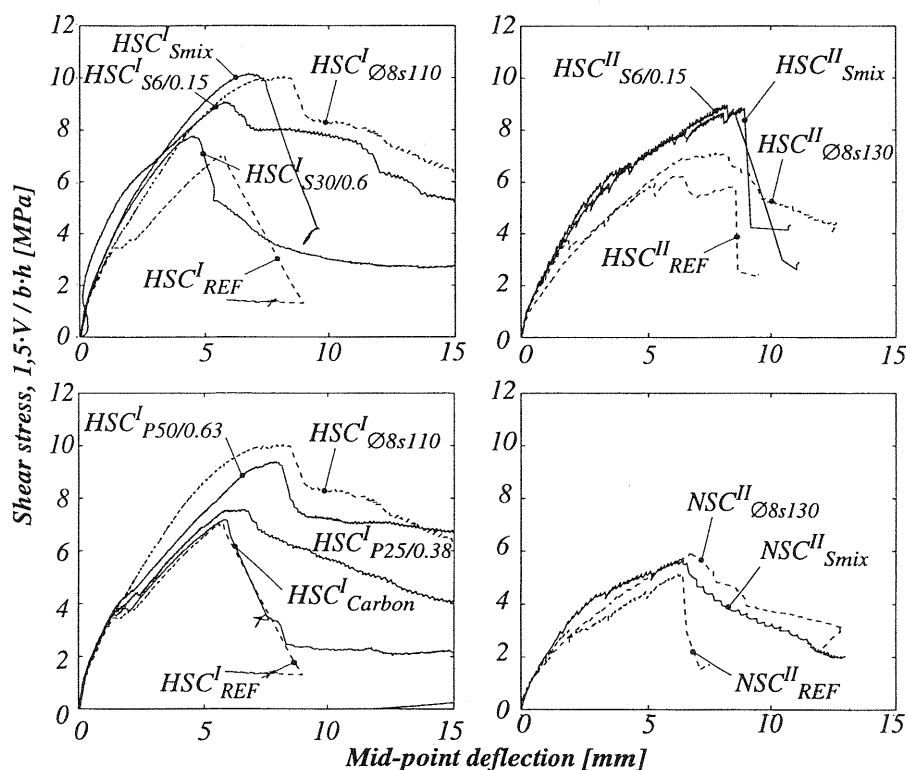


Fig. 2. Results of beam tests. Non-fibrous concretes are given by dashed lines.

### 3 Computational analysis - Truss model

The experimental observations inspire use of a truss analogy. The truss consists of compression and tension flanges and web members. The tension flange incorporates the reinforcement bars. Due to the bonding action between the rebars and concrete, the composite shows higher stiffness compared with the response of a bare rebar. This effect is called tension stiffening. There are similitudes in formation of cracks on the beams and on such composite tie-elements. Noghabai (1997) performed experiments on tie-elements made from the same concrete batches as the beams of series I, see Fig. 4a. The average distance between the cracks,  $s$ , in both beams and the tie-elements was about 100 mm. The stable growth of the cracks in the tie-element is dependent on the  $\sigma_f$ - $w$  response, as it was said to be the case for the beam in general. An analytical model was developed, based on the stress-strain relationship of the rebar and the  $\sigma_f$ - $w$  curve of the concrete (Noghabai and Olofsson, 1998), see Fig. 4b. An incremental approach must be used to fulfil equations 1) and 2) in Fig. 4b, simultaneously. In Fig. 4c the analytical and experimental results are compared for three cases. Fig. 4c suggests that the tension stiffening effect is clearly a function of the  $\sigma_f$ - $w$  relationship. Thus, a model that accounts for the distributed cracks in a beam is established.

In a phenomenological approach, the distances between the flexural cracks in the beams defines the locations of the web members. The diagonal cracks recur with  $45^\circ$  inclination on all beams, between the fields with dominating tension and compression. A truss may be discretized according to Fig. 5 which comprises members: (a) compression flange, (b) tension flange, diagonal web in (c) tension and in (d) compression. The simplified model for tension stiffening according to Fig. 4, applies as constitutive law for the tension flange (b). Members (a), (c) and (d) soften in tension where the "plastic" softening strain is based on the crack opening,  $w$ , divided by the length of the member. Thus, a size effect is inherent in the model for the diagonal shear cracks. Due to lack of experimental results on the compression behaviour of concrete, all members abide by the stress-strain relation as recommended by CEB (1995). This constitutive law in compression is valid for all the elements.

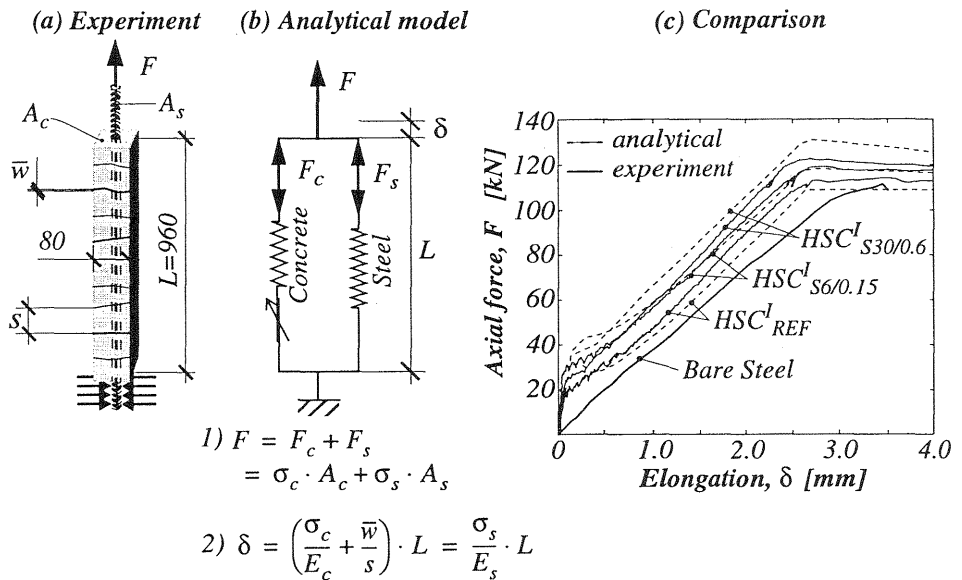


Fig. 4. Analytical modelling of a tie-element for use in the truss model.  $A$  = cross-section area,  $\sigma$  = stresses,  $E$  = modulus of elasticity,  $w$  = crack width, indices  $s$  and  $c$  stand for steel and concrete. Modified from Noghabai and Olofsson (1998).

Fig. 5 shows the model predictions for the  $HSC^I_{REF}$ ,  $HSC^I_{S6/0.15}$  and  $HSC^I_{Smix}$  beams. In Fig. 5 the relation between the predicted and experimental load carrying capacity are given within parenthesis. Beams of  $HSC^I_{REF}$  and  $HSC^I_{S6/0.15}$  failed in flexural-shear, i.e. the numerical collapse corresponds to a softening of the tensioned web members. The final failure for  $HSC^I_{Smix}$  occurred when the most strained member of the tensioned flange (b) started to yield. Prior to yielding almost all tensioned diagonal trusses had reached their softening branches. In the experiment the  $HSC^I_{Smix}$  beam failed in compression. At peak load, the model on this particular case gives a stress value amounting 85% of the compressive strength. The stress concentration caused by the loading plate is probably the main reason for the premature compressive failure in the experiment, hence the slightly higher model estimate. In Fig. 6 the distorted trusses are inlaid in the photographs of the authentic beams. Notice the correspondence between the crack spacing ( $s$ ) of the flexural cracks on the beam and the location of the web members in the model.

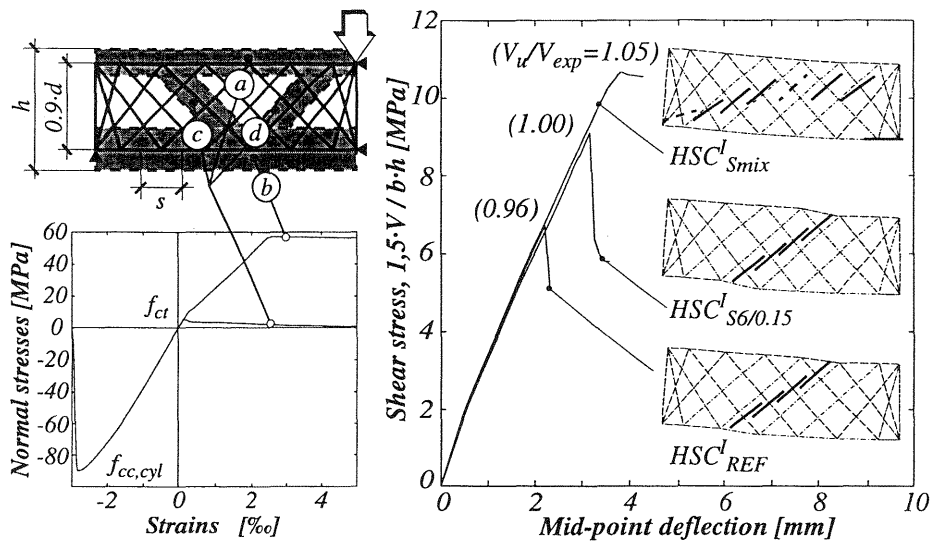


Fig. 5. Left: discretization of the beam and the adopted constitutive relations for the members of the truss model. Right: analytical results including modes of failure and crack orientation, cf. Fig. 2. Full lines in the distorted figures indicate softening or yielding and dashed lines symbolize unloading.

#### 4 Conclusions

In beams of the tested geometry, fibres for amounts of roughly 1% per volume concrete may substitute the shear reinforcement. Also, the structural stiffness may be enhanced (manifested by smaller crack widths on the beams) especially for steel fibres. The amount of fibres must be optimized with respect to beam dimensions in order to obtain not only a high shear capacity but also toughness in post-failure stage. Phenomenologically, failure of beams under transverse loading may be described by interaction of three zones in the beam: (1) the compression zone, (2) the web where tensile stresses act on the diagonal cracks and (3) the composite action of the rebars embedded in the concrete located in the tensioned part of the beam. The law for evolution of stable growth of cracks in the structure is based on uniaxial tensile tests. A nonlinear truss model was developed based on these assumptions. This simple model seems to capture the essentials of the experiments including the mechanisms of failure.



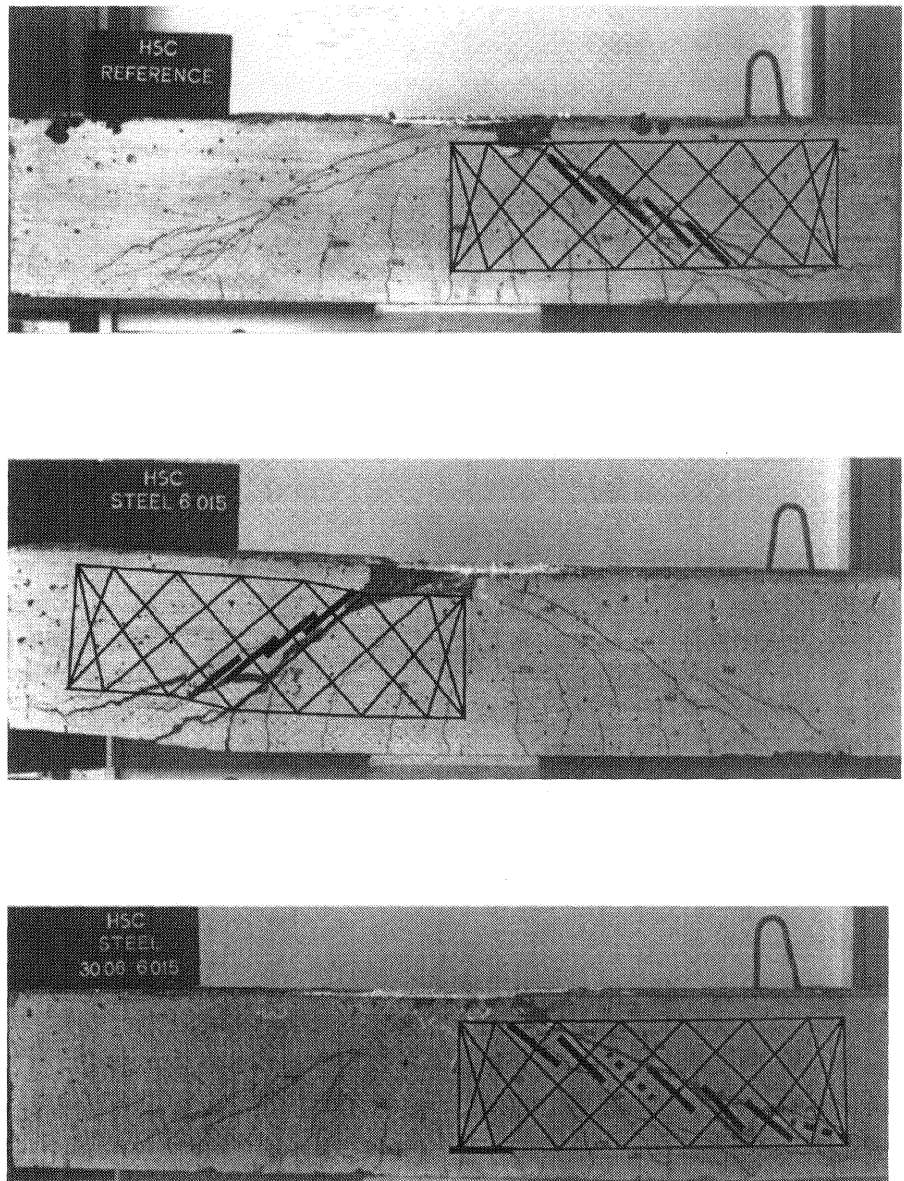


Fig. 6. Comparison between model prediction of the type of failure and the authentic cases (from up to down)  $HSC^I_{REF}$ ,  $HSC^I_{S6/0.15}$  and  $HSC^I_{Smix}$ .

## 5 Acknowledgement

This project has been supported by a consortium of Cementa AB, Euroc Beton AB, NCC AB, SKANSKA AB, Strängbetong AB, ELKEM AS, the Swedish Council for Building Research (BFR) and the Swedish National Board for Industrial and Technical Development (NUTEK). The research program was planned and conducted by Tech. lic. Noghabai and the analysis was done together with Dr. Olofsson. The work was supervised by Prof. Dr. Lennart Elfgren.

## 6 References

CEB (1995) High Performance Concrete, Recommended Extensions to the Model Code 90, Research Needs, **Bulletin d'Information No 228**, Comité Euro-International du Béton (CEB), Stuttgart.

Noghabai K. (1995) **Splitting of Concrete in the Anchoring Zone of Deformed Bars - A Fracture Mechanics Approach to Bond**, Licentiate Thesis 1995:26L, Luleå University of Technology, Div. Structural Engineering, Sweden.

Noghabai K. (1995) Splitting of concrete covers - A fracture mechanics approach, in **Fracture Mechanics of Concrete Structures** (ed. F.H. Wittman), AEDIFICATIO, 1575-1584.

Noghabai K. (1997) Effect of various types of fibers on the bond capacity - Experimental, analytical and numerical investigations, in **ACI Spring Convention**, Seattle (to be published).

Noghabai K. and Olofsson T. (1998) Effect of tension softening of concrete on the tension stiffening of rebars in plain and fibrous concrete, in this volume.

Noghabai K. (1998) **Effect of Tension Softening on the Performance of Concrete Structures - Experimental, Computational and Analytical Studies**, Ph.D. thesis, Luleå University of Technology, Div. Structural Engineering, (to be published).